Keggin structure. The previous studies involved V^{5+} substitution when the central heteroatom was Si, P, or B[8] and Pb^{2+} and Ti^{4+} substitution when the central atom was P.[25,39] The Pb^{2+} complex was atypical,[40] involving a temperature-dependent shift of the signal from W(4) far downfield from its position in the other complexes, owing presumably to some rapid exchange, possibly with the lacunary species, and to unusual steric placement of the Pb atom.[25] All the other complexes, including the present ones, show some remarkably similar, although not identical, features with respect to orders of chemical shifts. In all of the spectra, the most downfield line (most deshielded W's) is for W(1) (the pair of W's sharing edges with the substituted metal), while the most shielded or second most shielded W's are W(4), those sharing corners with the substituted metal. The order of line assignments for the present study of the Zn^{2+} complexes is most similar to that for the V^{5+} derivative of 11-tungstosilicate.

Acknowledgment. This research was aided by NSF Grant CHE-8406088, by Grant CCB-8504039 from the U.S.–Spain Joint Committee for Scientific Cooperation, and by an instrument grant from the W. M. Keck Foundation. Parts of the work on substituted α_2 Wells–Dawson derivatives were supported at the University of Oregon by NSF Grant CHE-8612924.

---

(39) Knoth, W. H.; Domaille, P. J.; Roe, D. C. *Inorg. Chem.* **1983**, *22*, 198.

(40) Tourné, G. F.; Tourné, C. M.; Schouten, A. *Acta Crystallogr., Sect. B: Struct. Crystallogr. Cryst. Chem.* **1982**, *B38*, 1414.

Complexes of (Arylimido)vanadium(V). Synthetic, Structural, Spectroscopic, and Theoretical Studies of $V(Ntol)Cl_3$ and Derivatives

David D. Devore,[†] Joseph D. Lichtenhan,[†] Fusao Takusagawa,[‡] and Eric A. Maatta*[†]

Contribution from the Department of Chemistry, Kansas State University, Manhattan, Kansas 66506, and Department of Chemistry, University of Kansas, Lawrence, Kansas 66045. *Received March 23, 1987*

Abstract: The reactions of $VOCl_3$ with various para-substituted aryl isocyanates, p-XC_6H_4NCO (X = CH_3, CF_3, OCH_3, F, Cl, Br), afford the corresponding (arylimido)vanadium(V) trichloride species, $V(NC_6H_4X)Cl_3$. The p-tolylimido complex, $V(Ntol)Cl_3$, **1**, displays an extensive derivative chemistry. The reaction of **1** with Lewis bases affords monoaddition products such as $V(Ntol)Cl_3(THF)$ and $V(Ntol)Cl_3(PPh_3)$. The chloride ligands of **1** readily participate in nucleophilic substitution reactions, affording a range of alkoxide ($V(Ntol)Cl_{3-n}(O\text{-}t\text{-}Bu)_n$: $n = 1$, **2**; $n = 2$, **3**; $n = 3$, **4**), aryloxide ($V(Ntol)Cl_{3-n}(OAr)_n$: $n = 1$, **5**; $n = 2$, **6**; $n = 3$, **7**; Ar = 2,6-$C_6H_3(CH_3)_2$), and organometallic ($V(Ntol)Cl_{3-n}(CH_2SiMe_3)_n$: $n = 1$, **8**; $n = 2$, **9**; $n = 3$, **10**; $(\eta^5\text{-}C_5H_5)V(Ntol)Cl_2$, **11**) derivatives. The electronic spectra of complexes **1–10** each display an absorption in the near-IR region at ca. 1000 nm. Complexes **1–7** also display a second absorption in the visible region of the spectrum, and the energy of this absorption increases with increasing electronegativity of the basal ligand donor atoms. The ^{51}V NMR spectra of these (arylimido)vanadium(V) complexes have been determined; ^{51}V chemical shifts in this series span a range of 1700 ppm. The ^{51}V chemical shifts also correlate with the electronegativity of the basal ligand donor atoms. The lowest field position is observed for **10** ($\delta(^{51}V) = +1048$), and a regular progression of $\delta(^{51}V)$ to higher field occurs as the purely σ-donating alkyl groups are replaced by ligands of increased electronegativity and increased π-donating ability. The observed correlations of the electronic and ^{51}V NMR spectra with the chemical constitutions of complexes **1–10** are explained in terms of a dominating paramagnetic shielding contribution. Extended Hückel calculations on several model complexes are used to provide an explanation of the electronic factors underlying the disparate ^{51}V chemical shifts observed for complexes **1–10** and related vanadium(V) complexes bearing oxo and alkylimido ligands. An X-ray crystal structure determination reveals that complex **6** possesses a dimeric structure in the solid state. Each vanadium atom in the centrosymmetric dimer is coordinated in a trigonal-bipyramidal geometry, with a terminal tolylimido ligand and a bridging aryloxide group occupying the apical sites. There is a decided asymmetry in the V–O–V bridge bonding. Crystal data for **6**: monoclinic, $I2/c$; $a = 24.937$ (5), $b = 10.790$ (2), $c = 16.662$ (3) Å; $\beta = 97.18$ (2)°; $Z = 8$.

Although a number of vanadium(V) organoimido complexes are now known,[1] these species are generally insular and lack a systematic derivative chemistry. We now report that trichloro(p-tolylimido)vanadium(V), $V(Ntol)Cl_3$,[2] can be readily functionalized to afford a variety of alkoxide, aryloxide, and organometallic derivatives of (p-tolylimido)vanadium(V). The wide range of compounds accessible in this series has allowed us to begin to delineate the influence of various coordination environments on the ^{51}V NMR characteristics of (organoimido)vanadium(V) complexes. Correlations between the ^{51}V NMR results and the electronic spectra of these species are examined with the aid of extended Hückel calculations and provide an illustrative comparison to related vanadium(V) complexes of oxo and alkylimido ligands. We also report the molecular structure of a dimeric (2,6-dimethylphenoxide) species, $[V(Ntol)(OAr)_2Cl]_2$. A subsequent paper will describe various chelate derivatives of $V(Ntol)Cl_3$ and the preparations of (p-tolylimido)vanadium(IV) species.[3]

[†] Kansas State University.

[‡] University of Kansas.

(1) (a) Burger, H.; Smrekar, O.; Wannagat, U. *Monatsh. Chem.* **1964**, *95*, 292. (b) Slawisch, A. *Z. Anorg. Allg. Chem.* **1970**, *374*, 291. (c) Shihada, A. F. *Z. Anorg. Allg. Chem.* **1974**, *408*, 9. (d) Nugent, W. A.; Harlow, R. L. *J. Chem. Soc., Chem. Commun.* **1979**, 342. (e) Preuss, F.; Towae, W. *Z. Naturforsch., B: Anorg. Chem., Org. Chem.* **1981**, *36B*, 1130. (f) Bradley, D. C.; Hursthouse, M. B.; Jelfs, A. N. M.; Short, R. L. *Polyhedron* **1983**, *2*, 849. (g) Nugent, W. A. *Inorg. Chem.* **1983**, *22*, 965. (h) Preuss, F.; Towae, W.; Kruppa, V.; Fuchslocher, E. *Z. Naturforsch., B: Anorg. Chem., Org. Chem.* **1984**, *39B*, 1510. (i) Schweda, E.; Scherfise, K. D.; Dehnicke, K. *Z. Anorg. Allg. Chem.* **1985**, 117. (j) Preuss, F.; Becker, H. *Z. Naturforsch., B: Anorg. Chem., Org. Chem.* **1986**, *41B*, 185. (k) Preuss, F.; Noichl, H.; Kaub, J. *Ibid.* **1986**, *41B*, 1085.

(2) Maatta, E. A. *Inorg. Chem.* **1984**, *23*, 2560.

(3) Wheeler, D. E.; Maatta, E. A., to be submitted for publication.

0002-7863/87/1509-7408$01.50/0

Results

Syntheses and Properties. The synthesis of V(Ntol)Cl_3, **1**, from $VOCl_3$ and *p*-tolyl isocyanate is readily accomplished in refluxing octane. A range of para-substituted phenylimido derivatives may be similarly prepared by using the appropriate aryl isocyanate as shown in eq 1. All of these (arylimido)vanadium(V) species are intensely colored solid materials that decompose rather quickly upon exposure to the atmosphere; they can, however, be stored at room temperature under nitrogen for extended periods of time. These trichloro complexes are moderately soluble in benzene and toluene, are considerably more soluble in methylene chloride and chloroform, and are quite soluble in coordinating solvents such as tetrahydrofuran. All of these species display excellent thermal stability: V(Ntol)Cl_3 may be conveniently purified by sublimation at ca. 130 °C (10^{-4} Torr). The mass spectrum of **1** determined at 35 °C reveals only mononuclear isotopomers to be present. The structure of **1** in the solid state is not known; however, the degree of oligomerization of related imidovanadium(V) systems varies with the nature of the imido substituent. For example, while $V(NSiMe_3)Cl_3$ is monomeric in the solid state,[1i] $V(NI)Cl_3$ is dimeric with bridging chloride ligands.[4] The related complex $V(NPh)Cl_3$ is polymeric (with weak chloride bridges) in the solid state.[5] V(Ntol)Cl_3 undergoes a color change from dark purple to green upon dissolution in toluene; this observation most likely reflects an oligomeric $[V(Ntol)Cl_3]_x$ species dissociating into monomeric units in solution.

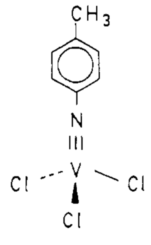

1

$$OVCl_3 + p\text{-}XC_6H_4NCO \xrightarrow[\text{reflux}]{\text{octane}} V(NC_6H_4X)Cl_3 + CO_2 \quad (1)$$

$$X = CH_3,\ CF_3,\ OCH_3,\ F,\ Cl,\ Br$$

V(Ntol)Cl_3 possesses a formal 12-electron configuration and reacts readily with Lewis bases such as THF or PPh_3 to afford isolable addition complexes of the form V(Ntol)Cl_3(L). The isolation of these monoadducts is somewhat surprising in view of the chemistry displayed by the isoelectronic $VOCl_3$ system, which typically forms bisadducts of the type $VOCl_3(L)_2$.[6] It seems likely that pseudooctahedral bisadducts of the type V(Ntol)$Cl_3(L)_2$ can form in solution, and their instability to isolation may be attributable to the strong trans-influence exerted by organoimido ligands in 16-electron pseudooctahedral complexes.[7] It is also probable that the nature of the organoimido substituent influences the degree of Lewis base association in V(NR)Cl_3 species.

The chloride ligands in V(Ntol)Cl_3 may be sequentially substituted by stoichiometric amounts of potassium *tert*-butoxide in THF solution to afford purple V(Ntol)Cl_2(O-*t*-Bu), **2**, orange V(Ntol)Cl$(O\text{-}t\text{-}Bu)_2$, **3**, and yellow V(Ntol)$(O\text{-}t\text{-}Bu)_3$, **4**, as shown in eq 2. In the ^1H NMR spectra of these organoimido alkoxides, the resonances due to the aryl protons, the tolyl methyl group, and the O-*t*-Bu protons all shift to progressively higher fields as the degree of substitution increases, presumably reflecting increasing electronic saturation provided by the strongly π-donating *tert*-butoxide groups.

$$V(Ntol)Cl_3 + n\text{KO-}t\text{-Bu} \xrightarrow{\text{THF}} V(Ntol)Cl_{3-n}(O\text{-}t\text{-Bu})_n \quad (2)$$

$$\mathbf{2}\ (n = 1);\ \mathbf{3}\ (n = 2);\ \mathbf{4}\ (n = 3)$$

Likewise, an homologous series of 2,6-dimethylphenoxide derivatives of **1** has been prepared, as shown in eq 3–5 (Ar = 2,6-$C_6H_3(CH_3)_2$). Aryloxide ligands are less efficient π donors than are alkoxide ligands, and thus the vanadium centers in the 2,6-dimethylphenoxide complexes should be relatively electron deficient as compared to their *tert*-butoxide analogues. The comparative electrophilicity of the aryloxide species is readily apparent in their ^{51}V NMR spectra (vide infra) and is also manifest in the constitution of the mono- and bis(2,6-dimethylphenoxide) complexes: unlike the corresponding *tert*-butoxide species, the mono(aryloxide) complex incorporates a ligating THF molecule and the bis(aryloxide) complex adopts a dimeric structure in which the vanadium atoms are bridged by two dimethylphenoxide ligands.

$$\mathbf{1} + HOAr \xrightarrow{\text{THF}} \underset{\mathbf{5}}{V(Ntol)Cl_2(OAr)(THF)} \quad (3)$$

$$\mathbf{1} + HOAr\ (\text{excess}) \xrightarrow{\text{THF}} \underset{\mathbf{6}}{[V(Ntol)Cl(OAr)(\mu\text{-}OAr)]_2} \quad (4)$$

$$\mathbf{1} + 3HOAr \xrightarrow[\text{Et}_3\text{N}]{\text{THF}} \underset{\mathbf{7}}{V(Ntol)(OAr)_3} \quad (5)$$

All of the dimethylphenoxide complexes are very soluble in common organic solvents, including pentane, which renders them difficult to crystallize. As is the case with all of the organoimido complexes reported herein, exposure of the dimethylphenoxide derivatives to air results in their rapid decomposition, presumably via extensive hydrolysis. We have studied the controlled hydrolysis of V(Ntol)$(OAr)_3$ by ^1H and ^{51}V NMR. Addition of H_2O (1 equiv) to a C_6D_6 solution of **7** results in relatively clean hydrolysis of the tolylimido ligand, forming *p*-toluidine and $OV(OAr)_3$ ($\delta(^{51}V) = -511$; fwhm = 20 Hz), along with a small amount of free 2,6-dimethylphenol, without any detectable intermediates (eq 6).

$$\mathbf{7} + H_2O \rightarrow OV(OAr)_3 + tolNH_2 \quad (6)$$

The identity of the $OV(OAr)_3$ product has been confirmed by an X-ray crystal structure analysis.[8] Similarly, the controlled hydrolysis of $[V(Ntol)Cl(OAr)_2]_2$ in C_6D_6 affords *p*-toluidine and $OVCl(OAr)_2$ ($\delta(^{51}V) = -363$; fwhm = 54 Hz); significant amounts of $OV(OAr)_3$ and free 2,6-dimethylphenol were also observed in the NMR spectra of this reaction.

An homologous series of (trimethylsilyl)methyl complexes has also been prepared as shown in eq 7. Although a variety of alkylating agents were examined (including RLi, RMgX, and R_2Zn reagents), tractable alkyl complexes of (tolylimido)vanadium(V) were only obtained by using bis[(trimethylsilyl)-methyl]magnesium. Complexes **8**–**10** are rare examples of vanadium(V) organometallics;[9] it seems likely that our inability to isolate organometallic vanadium(V) derivatives from the reactions

$$\mathbf{1} + Mg(CH_2SiMe_3)_2 \xrightarrow[0\ ^\circ C]{\text{toluene}} V(Ntol)(CH_2SiMe_3)_xCl_{3-x} \quad (7)$$

$$\mathbf{8}\ (x = 1);\ \mathbf{9}\ (x = 2);\ \mathbf{10}\ (x = 3)$$

---

(4) Beindorf, G.; Strähle, J.; Liebelt, W.; Weller, F. *Z. Naturforsch., B: Anorg. Chem., Org. Chem.* **1980**, *36B*, 153.

(5) Bradley, D. C.; Jelfs, A. N. M., personal communication.

(6) Funk, H.; Weiss, W.; Zeising, M. *Z. Anorg. Allg. Chem.* **1958**, *296*, 36.

(7) Chou, C. Y.; Huffman, J. C.; Maatta, E. A. *Inorg. Chem.* **1986**, *25*, 822.

(8) Devore, D. D.; Takusagawa, F.; Maatta, E. A., unpublished results.

(9) Apart from our CpV(Ntol)Cl_2 and V(Ntol)$(CH_2SiMe_3)_xCl_{3-x}$ species, the only well-characterized vanadium(V) organometallics known to us are the following. (a) $CpVOX_2$ (X = Cl, Br): de Liefde Meyer, H. J.; Van der Kerk, G. J. M. *Recl. Trav. Chim. Pays-Bas* **1965**, *84*, 1418. (b) $VO(CH_2SiMe_3)_3$: Mowat, W.; Shortland, A.; Yagupsky, G.; Hill, N. J.; Yagupsky, M.; Wilkinson, G. *J. Chem. Soc., Dalton Trans.* **1972**, 533. (c) $VO(OR)_2CH_3$ (R = *i*-Pr, *s*-Bu, *t*-Bu): Lachowicz, A.; Thiele, K.-H. *Z. Anorg. Allg. Chem.* **1977**, *431*, 88. (d) Cp_2VOCl: Holliday, A. K.; Makin, P. H.; Puddephatt, R. J. *J. Chem. Soc., Dalton Trans.* **1979**, 228. (e) $VO(O\text{-}i\text{-}Pr)_2Ph$: Choukroun, R.; Sabo, S. *J. Organomet. Chem.* **1979**, *182*, 221. (f) $VOCl_2Ph$: Thiele, K.-H.; Schumann, W.; Wagner, S.; Bruser, W. *Z. Anorg. Allg. Chem.* **1972**, *390*, 280. (g) Li[VO(O-*t*-Bu)$_3$(*n*-Bu)], VO(O-*t*-Bu)$_2$(CH_2SiMe_3): Preuss, F.; Ogger, L. *Z. Naturforsch., B: Anorg. Chem., Org. Chem.* **1982**, *37B*, 957. (h) VOR_3 (R = mesityl): Seidel, W.; Kreisel, G. *Z. Chem.* **1982**, *22*, 113. (i) V(N-*t*-Bu)(O-*t*-Bu)$_2$R (R = Me, *n*-Bu, CH_2SiMe_3, mesityl), V(N-*t*-Bu)(O-*t*-Bu)R_2 (R = mesityl): Reference 1j. (j) $(C_5R_5)VOX_2$ (R = H, CH_3; X = Cl, Br, Ph, OCH_3): Herrmann, W. A.; Weichselbaumer, G.; Kneuper, H.-J. *J. Organomet. Chem.* **1987**, *319*, C21.

Table I. Electronic Spectra of $V(Ntol)Cl_3$ and Derivatives[a]

complex	λ_{max}, nm vis	near-IR
$V(Ntol)Cl_3$ (**1**)	654	1040
$V(Ntol)Cl_2(O\text{-}t\text{-}Bu)$ (**2**)	516	1052
$V(Ntol)Cl(O\text{-}t\text{-}Bu)_2$ (**3**)	432	960
$V(Ntol)(O\text{-}t\text{-}Bu)_3$ (**4**)	399	891
$V(Ntol)Cl_2(OAr)(THF)$ (**5**)[b]	434	1028
$[V(Ntol)Cl(OAr)_2]_2$ (**6**)[b]	411	980
$V(Ntol)(OAr)_3$ (**7**)[b]	390	977
$V(Ntol)Cl_2(CH_2SiMe_3)$ (**8**)		1000
$V(Ntol)Cl(CH_2SiMe_3)_2$ (**9**)		1000
$V(Ntol)(CH_2SiMe_3)_3$ (**10**)		1055

[a] Toluene solution; 23 C. [b] Ar = 2,6-$C_6H_3(CH_3)_2$.

Table II. ^{51}V NMR Data for $V(Ntol)Cl_3$ and Related Complexes[a]

complex	$\delta(^{51}V)$	fwhm, Hz	$^1J_{^{51}V-^{14}N}$, Hz
$V(Ntol)(CH_2SiMe_3)_3$[e]	1048	270[b]	94
$V(Ntol)Cl(CH_2SiMe_3)_2$[e]	900	353	
$V(Ntol)Cl_2(CH_2SiMe_3)$[e]	697	378	
$V(Ntol)Cl_3(PPh_3)$	392	700	
$V(Ntol)Cl_3(THF)$	374	1900	
$V(Ntol)Cl_3$	305	500	
$V(Ntol)Cl_2(OC_6H_3Me_2)(THF)$	77	1170	
$V(Ntol)Cl_2(O\text{-}t\text{-}Bu)$	−171	500	
$[V(Ntol)Cl(OC_6H_3Me_2)_2]_2$	−231[d]	463	
$V(Ntol)(\eta^5\text{-}C_5H_5)Cl_2$	−240	790	
$V(Ntol)(OC_6H_3Me_2)_3$	−428	366[b]	98
$V(Ntol)Cl(O\text{-}t\text{-}Bu)_2$	−472	390	
$V(Ntol)(O\text{-}t\text{-}Bu)_3$	−654	90[c]	111

[a] $CDCl_3$ solution, 298 K, 105.2 MHz, relative to external $VOCl_3$/$CDCl_3$ (75% v/v). Positive values denote downfield chemical shifts. [b] Partially resolved 1:1:1 triplet. [c] Fully resolved 1:1:1 triplet. [d] The chemical shift for this species is concentration dependent, ranging from δ −239 for a saturated $CDCl_3$ solution to δ −223 upon ~2-fold dilution of the former solution. [e] C_6D_6 solution.

of $V(Ntol)Cl_3$ with alkylating agents other than $Mg(CH_2SiMe_3)_2$ was due to reduction to paramagnetic V(IV) species.[9g] The (trimethylsilyl)methyl complexes are all orange, oily materials that are extremely soluble in common organic solvents, including pentane. They are only moderately stable at room temperature: noticable decomposition is observed for **8** within hours, for **9** within several days, and for **10** within several weeks. These decompositions are accelerated by light. In the ^1H NMR spectra of these species, the protons of the vanadium-bound methylene groups give rise to broadened resonances with line widths ranging from 14 Hz in the case of **8** to 53 Hz in the case of **10**. This broadening may result from interaction with the vanadium quadrupole or from unresolved spin coupling ($^2J_{^{51}V-^1H}$ has been reported to be ca. 12 Hz in complexes of the type $OV(O\text{-}t\text{-}Bu)_2R$[9g]).

$V(Ntol)Cl_3$ reacts cleanly with $Me_3SiC_5H_5$ to produce the (η^5-cyclopentadienyl)vanadium(V) derivative $CpV(Ntol)Cl_2$, **11**, as shown in eq 8. **11** is obtained as a microcrystalline brown-black

$$\mathbf{1} + Me_3SiC_5H_5 \xrightarrow{CH_2Cl_2} \underset{\mathbf{11}}{CpV(Ntol)Cl_2} + Me_3SiCl \quad (8)$$

solid that is stable at room temperature under an inert atmosphere. **11** may also be synthesized from the reaction of **1** with sodium cyclopentadienide in THF. Attempts to introduce a second cyclopentadienyl ligand to afford $Cp_2V(Ntol)Cl$ were unsuccessful.

Electronic Spectroscopy. The electronic spectra of complexes **1**–**10** were recorded as toluene solutions throughout the range 380–1400 nm. The results are presented in Table I. All of the complexes display an absorption in the near-IR region at ca. 1000 nm. For the three (trimethylsilyl)methyl complexes (**8**–**10**), this absorption is much broader than for the other species listed in Table I. For complexes **1**–**7**, a second absorption in the visible region is also observed. Unlike the transitions in the near-IR region, the band maxima for these absorptions display a considerable variance in energy, which is seen to correlate with the electronegativity (or π-donation ability) of the basal ligand set donor atoms. Successive replacement of the chloride ligands of $V(Ntol)Cl_3$ by either *tert*-butoxide or 2,6-dimethylphenoxide ligands induces a progressive shift in the visible region absorption toward higher energy. For the alkyl complexes, **8**–**10**, no distinct absorption maxima in the visible region of the spectrum were observed; the orange color of complexes **8**–**10** derives from the "tail" of an absorption in the UV region of the spectrum (a feature common to all of the complexes **1**–**10**). Considering the above band energy/ligand electronegativity relationship, it is reasonable to expect that the corresponding electronic transition for complexes **8**–**10** would appear in the near-IR region of the spectrum. This suggestion is in accord with the observed breadth of the absorption near 1000 nm in the spectra of **8**–**10**.

We assign the low-energy, near-IR absorption to a $\pi \rightarrow \pi^*$ transition involving the electrons of the V–N multiple bond. Given the fact that the *p*-tolylimido group is common to all of the complexes listed in Table I, it is reasonable to expect that the energies associated with this $\pi \rightarrow \pi^*$ transition should not vary greatly with changes in the basal ligand set. We assign the second, higher energy absorption to a transition involving electrons associated with the monoanionic ligands. Given the range of electronegativities of the donor atoms of the basal ligands, a comparatively wide variance in the energy of such transitions is to be expected, in accord with our observations. As will be discussed in a later section, these assignments are supported by extended Hückel calculations.

^{51}V NMR Spectroscopy. ^{51}V is an appealing nucleus for NMR studies, owing to the favorable combination of its high natural abundance (99.76%), high sensitivity (0.382 relative to that of ^1H at equal field strength), and low electric quadrupole moment ($Q = -0.05b$). Thus, ^{51}V NMR resonances are readily observable even for magnetically dilute samples, data acquisition is rapid, and line widths are relatively small even for complexes of low symmetry. With few exceptions,[1h,10] previous ^{51}V NMR studies of vanadium(V) species in solution have concerned oxovanadium complexes. A large body of data on these systems has been accumulated, and the field has been recently reviewed by Rehder.[11,12]

^{51}V NMR data for the (*p*-tolylimido)vanadium(V) complexes prepared herein are collected in Table II. The ^{51}V chemical shifts for these species span a range of 1700 ppm; the lowest field resonance in this group is found for $V(Ntol)(CH_2SiMe_3)_3$ (δ 1048), and a regular progression of the chemical shifts to higher field is seen as the purely σ-donating alkyl groups are sequentially replaced by ligands of increased electronegativity and π-donating ability. The ^{51}V chemical shifts of these (*p*-tolylimido)vanadium(V) species thus follow the so-called "inverse halogen dependence", in which the nuclei become increasingly shielded as the electronegativity of the substituents is increased. This behavior was first noted for vanadium(V) complexes by Rehder,[13,14] who found that the shielding in oxovanadium(V) species increased in the order $VOBr_3$ (δ +432) < $VOCl_3$ (δ 0) < VOF_3 (δ −632). The downfield chemical shifts of $V(Ntol)Cl_3$ and its (trimethylsilyl)methyl derivatives are highly unusual in ^{51}V NMR spectroscopy: the great majority of all other vanadium species studied in solution give rise to resonances upfield of the $VOCl_3$ reference. The resonances due to $V(Ntol)(CH_2SiMe_3)_3$, $V(Ntol)(O\text{-}2,6\text{-}C_6H_4(Me)_2)_3$, and $V(Ntol)(O\text{-}t\text{-}Bu)_3$ were sufficiently narrow to allow resolution of vanadium–nitrogen spin coupling, with $^1J_{^{51}V-^{14}N}$ values of 94, 98, and 111 Hz, respectively. These values compare well with those previously reported for $VO(NEt_2)(O\text{-}i\text{-}Pr)_2$ (105 Hz),[14,15] $V(N\text{-}t\text{-}Bu)(OSiMe_3)_3$ (95 Hz),[1d] and several (alkylimido)vanadium(V) alkoxide derivatives (92–112 Hz).[1h]

---

[10] Harrison and Howarth have recently reported a ^{51}V NMR study of various sulfidovanadates, including $[VS_4]^{3-}$ and $[V_2S_4]^{4-}$: Harrison, A. T.; Howarth, O. W. *J. Chem. Soc., Dalton Trans.* **1986**, 1405.

[11] Rehder, D. *Magn. Reson. Rev.* **1984**, *9*, 125.

[12] Rehder, D. *Bull. Magn. Reson.* **1982**, *4*, 33.

[13] Rehder, D. *Z. Naturforsch., B: Anorg. Chem., Org. Chem.* **1977**, *32B*, 771.

[14] Priebsch, W.; Rehder, D. *Inorg. Chem.* **1985**, *24*, 3058.

[15] Hoch, M.; Rehder, D.; Weidemann, C. *Inorg. Chim. Acta* **1984**, *92*, L5.

Table III. Comparison of ^{51}V NMR Data for Oxo- and (*p*-Tolylimido)vanadium(V) Species

complex	$\delta(^{51}V)$	fwhm, Hz
$V(Ntol)Cl_3$[a]	305	500
$VOCl_3$	0	23
$V(Ntol)Cl_2(O\text{-}t\text{-}Bu)$[a]	−171	500
$VOCl_2(O\text{-}t\text{-}Bu)$[b,c]	−328	19
$V(Ntol)Cl(O\text{-}t\text{-}Bu)_2$[a]	−472	390
$VOCl(O\text{-}t\text{-}Bu)_2$[b,c,d]	−537	24
$V(Ntol)(O\text{-}t\text{-}Bu)_3$[a]	−654	90
$VO(O\text{-}t\text{-}Bu)_3$[b,c,d]	−669	12
$[V(Ntol)Cl(OC_6H_3Me)_2]_2$[a]	−227	463
$VOCl(OC_6H_3Me_2)_2$[a]	−363	54
$V(Ntol)(OC_6H_3Me_2)_3$[a]	−428	366
$VO(OC_6H_3Me_2)_3$[a]	−511	20
$V(Ntol)(\eta^5\text{-}C_5H_5)Cl_2$[a]	−240	790
$VO(\eta^5\text{-}C_5H_5)Cl_2$[e]	−393	50

[a] This work. [b] From ref 14. [c] From ref 12. [d] From ref 9g. [e] From ref 9h.

Table IV. ^{51}V NMR Data for Para-Substituted (Arylimido)vanadium(V) Trichlorides, $V(NC_6H_4X)Cl_3$[a]

complex	$\delta(^{51}V)$	fwhm, Hz
$V(NC_6H_4OCH_3)Cl_3$	403	730
$V(NC_6H_4CH_3)Cl_3$	305	500
$V(NC_6H_4F)Cl_3$	258	370
$V(NC_6H_4Cl)Cl_3$	253	525
$V(NC_6H_4Br)Cl_3$	251	610
$V(NC_6H_4CF_3)Cl_3$	182	500

[a] $CDCl_3$ solution, 298 K, 105.2 MHz, relative to external $VOCl_3/CDCl_3$ (75% v/v).

Table III provides a comparison of ^{51}V NMR data available for pairs of analogous oxo- and (*p*-tolylimido)vanadium(V) complexes. In all cases, the line width of a particular tolylimido species is larger than that observed for the corresponding oxo complex. The presence of vanadium–nitrogen spin coupling undoubtedly contributes significantly to the breadth of the resonances for the tolylimido complexes. An additional contribution to larger line widths can be expected to result from enhanced quadrupolar broadening induced by the lowering of symmetry upon replacement of a cylindrical vanadyl unit with a planar V(Ntol) group. It is also apparent in Table III that the ^{51}V chemical shift of a particular tolylimido complex is always found downfield of that observed for its oxo analogue and that the magnitude of the disparity decreases as additional π bonding, increasingly electronegative ligands are introduced into the vanadium coordination sphere. The relative ordering of the chemical shifts of these oxo- and (*p*-tolylimido)vanadium(V) complexes (i.e., $\delta(V(Ntol)Z_3) < \delta(VOZ_3)$) again follows the inverse halogen dependence; a similar trend can be seen in the (solid-state) ^{51}V NMR spectra of the tetrahedral vanadium–chalcogen trianions: $\delta(VTe_4^{3-}) < \delta(VSe_4^{3-}) < \delta(VS_4^{3-})$.[16]

As shown in Table IV, the ^{51}V chemical shifts of (arylimido)vanadium(V) trichloride species are quite sensitive to the nature of the para substituent borne by the aryl ring. The six entries in Table IV span a chemical shift range of ca. 220 ppm, with the strongly electron-donating *p*-methoxy derivative appearing at the lowest field position and the strongly electron-withdrawing *p*-trifluoromethyl derivative giving rise to the highest field position. Both σ (inductive) and π (resonance) effects are contributory factors in determining the chemical shift of a particular arylimido complex. This can be seen by referring to Table V, wherein group substituent constants, separated into resonance and inductive contributions,[17] are tabulated for the six para substituents studied. When these σ_R and σ_I values are combined, the sums (Table V) correlate well with the observed ^{51}V chemical shifts of the appropriate arylimido complex (Table IV). Thus, the concept of an inverse halogen dependence can also be applied to the ^{51}V chemical shifts in this series: increasing the electron-withdrawing capability of the para substituent in the arylimido group has the effect of making the nitrogen donor atom more electronegative (i.e., more "oxo-like") and is manifest in an increased ^{51}V nuclear shielding.

Table V. Group Substituent Constants for Resonance and Inductive Effects[a]

X	σ_R	σ_I	$\sigma_R + \sigma_I$
OCH_3	−0.51	+0.17	−0.34
CH_3	−0.11	−0.05	−0.16
F	−0.44	+0.52	+0.08
Cl	−0.24	+0.47	+0.23
Br	−0.22	+0.45	+0.23
CF_3	+0.09	+0.41	+0.50

[a] From ref 17.

Table VI. Crystal Data for $[V(Ntol)Cl(O\text{-}2,6\text{-}C_6H_3Me_2)_2]_2$

formula	$C_{23}H_{25}NO_2ClV$
formula wt	433.85
a, Å	24.937 (5)
b, Å	10.790 (2)
c, Å	16.662 (3)
β, deg	97.18 (2)
V, Å^3	4448 (1)
Z	8
space gp	*I*2/*c*
cryst size, mm	0.5 × 0.3 × 0.1
radiation	Mo Kα, λ = 0.71069, monochromatized with highly oriented graphite
d_{calcd}, g/cm^3	1.296
temp, °C	25 (2)
μ, cm^{-1}	6.0987
scan range	1.3° below Kα_1 to 1.3° above Kα_2
scan speed, deg/min	1.5–20.0
bkgd measurements	$^1/_6$ of total scan at both edges
2θ limits, deg	4.0–42.0
no. of octants measd	2
total no. of reflcns	2481
no. of unique reflcns	2293
no. of variables	253
$R(F)$	0.0571
$R_w(F)$	0.0589

Two examples of (alkylimido)vanadium(V) trichlorides, (*t*-BuN)VCl_3 and (*i*-PrN)VCl_3, have been examined by ^{51}V NMR by Preuss et al.[1h] The ^{51}V chemical shifts for these species are very close to that of the $VOCl_3$ reference with values of δ +8 for the former and δ +21 for the latter. The occurrence of these resonances at relatively high field (as compared to their arylimido analogues) was initially a source of puzzlement to us; in the context of the inverse halogen dependence and the group electronegativity correlation developed above, our intuition led us to expect that the ^{51}V chemical shifts for these alkylimido species should occur further downfield than those of the corresponding $V(NAr)Cl_3$ species. The reasons for this apparent "anomaly" have been elucidated with the aid of extended Hückel calculations and will be addressed in the Discussion.

Structure of $[V(Ntol)Cl(O\text{-}2,6\text{-}C_6H_3Me_2)_2]_2$. Crystal data are summarized in Table VI, and a listing of fractional coordinates and isotropic thermal parameters is presented in Table VII. An ORTEP representation of the molecule is shown in Figure 1, while selected interatomic distances and angles are given in Table VIII.

Each vanadium atom in the centrosymmetric dimer is five-coordinate in a geometry that approximates that of a trigonal bipyramid, with the tolylimido ligand and a bridging aryloxide ligand occupying the apical sites. The bridging aryloxide ligands are arranged in a decidedly unsymmetrical fashion, with the axial V–O bond being 0.4 Å longer than the equatorial V–O bond. The V–V internuclear distance is 3.381 (2) Å, clearly indicating the absence of any bonding interaction between the metals. The structural features of $[V(Ntol)Cl(O\text{-}2,6\text{-}C_6H_3Me_2)_2]_2$ may be

---

[16] Becker, K. D.; Berlage, U. *J. Magn. Reson.* **1983**, *54*, 272.

[17] Taft, R. W., Jr.; Deno, N. C.; Skell, P. S. *Annu. Rev. Phys. Chem.* **1958**, *9*, 287.

Table VII. Fractional Coordinates and Isotropic Thermal Parameters[a] for $[V(Ntol)Cl(O\text{-}2,6\text{-}C_6H_3Me_2)_2]_2$

atom	*x*	*y*	*z*	*B*
V1	0.31736 (3)	0.27607 (6)	0.25996 (3)	4.46
Cl(2)	0.33862 (5)	0.2686 (1)	0.13336 (6)	6.28
N3	0.3732 (1)	0.2091 (3)	0.30179 (2)	5.12
O4	0.3256 (1)	0.4304 (2)	0.3004 (2)	5.24
O5	0.2674 (1)	0.1579 (2)	0.2891 (1)	4.36
C6	0.4222 (2)	0.1574 (4)	0.3329 (3)	5.78
C7	0.4680 (3)	0.2292 (5)	0.3546 (5)	8.94
C8	0.5175 (2)	0.1737 (5)	0.3796 (4)	8.05
C9	0.5210 (3)	0.0458 (6)	0.3891 (4)	9.01
C10	0.4749 (3)	−0.0250 (7)	0.3723 (5)	10.26
C11	0.4255 (2)	0.0291 (5)	0.3418 (5)	9.06
C12	0.5735 (2)	−0.0177 (6)	0.4199 (5)	10.35
C13	0.3688 (2)	0.4921 (4)	0.3369 (2)	5.26
C14	0.4008 (2)	0.5609 (5)	0.2908 (3)	6.95
C15	0.4458 (3)	0.6241 (7)	0.3288 (4)	9.51
C16	0.4571 (3)	0.6201 (6)	0.4130 (5)	9.77
C17	0.4248 (3)	0.5543 (6)	0.4593 (4)	9.08
C18	0.3788 (2)	0.4916 (4)	0.4212 (3)	7.42
C19	0.3851 (3)	0.5680 (5)	0.1995 (3)	9.83
C20	0.3446 (3)	0.4219 (7)	0.4762 (3)	9.70
C21	0.2813 (2)	0.0462 (3)	0.3234 (2)	4.53
C22	0.2897 (2)	−0.0551 (4)	0.2731 (2)	4.79
C23	0.3028 (2)	−0.1700 (4)	0.3070 (3)	5.87
C24	0.3065 (2)	−0.1865 (4)	0.3904 (3)	6.65
C25	0.2988 (2)	−0.0872 (4)	0.4401 (3)	6.35
C26	0.2867 (2)	0.0299 (4)	0.4063 (3)	5.93
C27	0.2888 (2)	−0.0440 (4)	0.1809 (3)	6.42
C28	0.2794 (3)	0.1386 (4)	0.4633 (3)	7.63

[a] $B = 8\pi^2\langle U\rangle$.

Table VIII. Selected Distances (Å) and Angles (deg) in $[V(Ntol)Cl(O\text{-}2,6\text{-}C_6H_3(CH_3)_2)_2]_2$

V1–Cl2	2.240 (1)	V1–V1′	3.381 (2)
V1–N3	1.644 (3)	N3–C6	1.384 (5)
V1–O4	1.797 (3)	O4–C13	1.346 (5)
V1–O5	1.888 (3)	O5–C21	1.360 (4)
V1–O5′	2.283 (3)		
Cl2–V1–N3	95.45 (2)	O4–V1–O5	125.24 (12)
Cl2–V1–O4	110.91 (9)	O4–V1–O5′	84.41 (11)
Cl2–V1–O5	117.35 (8)	O5–V1–O5′	72.04 (10)
Cl2–V1–O5′	89.52 (7)	V1–N3–C6	175.83 (32)
N3–V1–O4	101.38 (14)	V1–O4–C13	132.50 (26)
N3–V1–O5	98.37 (14)	V1–O5–C21	124.39 (23)
N3–V1–O5′	170.41 (14)		

accounted for in the following manner.[18] Five σ bonds can be formed utilizing the valence s, p_x, p_y, p_z, and d_{z^2} orbitals of vanadium. The metal d_{xz} and d_{yz} orbitals can overlap efficiently with the nitrogen p_x and p_y orbitals, leading to the formation of a formal V≡Ntol triple bond; this interaction is manifest in the near-linear V–N–C skeleton (175.8 (3)°) and the short V–N distance (1.644 (3) Å). The remaining metal orbitals, d_{xy} and $d_{x^2-y^2}$, are then available to engage in π bonding by accepting electron density from a filled, in-plane O 2p orbital on each of the equatorial aryloxide ligands. This bonding description nicely accounts for the unequal V–O bond distances in the aryloxide bridges since it allows for oxygen-to-vanadium π interaction only for the aryloxide ligands cis to the tolylimido group while O–V π bonding in the position trans to the tolylimido ligand is disfavored by virtue of competition with N–V π bonding. The long V–O distance trans to the tolylimido ligand suggests a rather weak bonding interaction, and it seems likely that this dimer is at least partially dissociated in solution. This suggestion is supported by our observations of (1) a modest dependence of $\delta(^{51}V)$ upon concentration and (2) a single phenoxide methyl resonance in the compound's ^1H NMR spectrum.

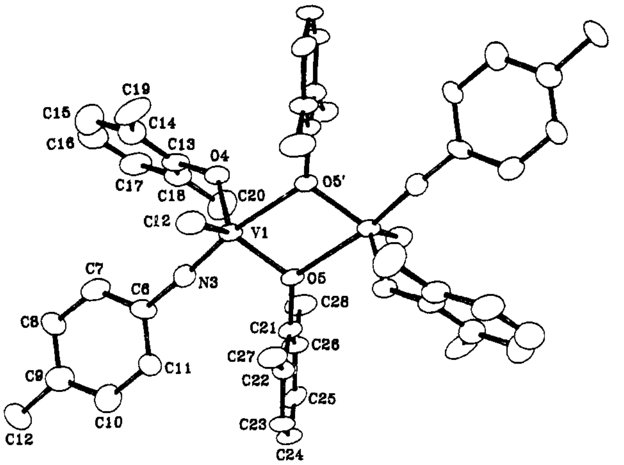

Figure 1. Molecular structure of $[V(Ntol)Cl(O\text{-}2,6\text{-}C_6H_3(CH_3)_2)_2]_2$, **6**.

Discussion

$V(Ntol)Cl_3$ provides a convenient entry point for the synthesis of a variety of (tolylimido)vanadium(V) species. The homologous series of alkyl, aryloxide, and alkoxide derivatives reported herein give rise to a wide range of ^{51}V NMR chemical shifts, and thus this family of compounds presents an attractive opportunity for examining the electronic factors underlying this broad chemical shift dispersion. A brief discussion of NMR theory[19] will serve as our starting point.

When negligible nonlocal diamagnetic contributions are ignored, the shielding constant for a particular vanadium nucleus can be expressed as a combination of a local diamagnetic contribution plus a local paramagnetic contribution, as in eq 9. The diamagnetic contribution to the overall nuclear shielding is dominated by field-induced motion of core electrons and can be regarded as being virtually invariant in ^{51}V NMR spectroscopy. For example, Nakano[20] has calculated σ_{dia} values for $[VO_4]^{3-}$ and $[V(CO)_6]^-$ as being 1708 and 1718 ppm, respectively; the congruency of these values, despite the drastic differences in oxidation state, geometry, and π-bonding capabilities of the ligands, justifies the assumption of a constant diamagnetic contribution.

$$\sigma = \sigma_{dia} + \sigma_{para} \tag{9}$$

Chemical shift differences in ^{51}V NMR spectroscopy therefore can be attributed to variations in the paramagnetic shielding term. For the general case of a first-row (3d) transition-metal ion, the paramagnetic contribution may be expressed[19,21] as in eq 10, where

$$\sigma_{para} = \frac{-e^2}{3m^2c^2}\sum_i (E_i - E_0)^{-1}\langle 0|\hat{L}^2|i\rangle\langle r^{-3}\rangle \tag{10}$$

E_0 is the ground-state energy, $\hat{L}$ is the angular momentum operator, r is the radius expectation value for the 3d electrons, and E_i is the energy of an excited state whose configuration transforms with the angular momentum operator. The paramagnetic shielding term in NMR spectroscopy is thus entirely analogous to the "temperature-independent paramagnetism" term encountered in magnetic susceptibility studies.[22,23] For complexes of high point group symmetry, only certain excited-state configurations will contribute to the paramagnetic shielding term; in the present case, however, the $V(Ntol)X_3$ compounds, which we shall examine, possess C_s symmetry and all excited-state configurations can contribute to σ_{para}.

---

(18) The related d^0 dimers $[W(N\text{-}t\text{-}Bu)_2(CH_3)_2]_2$ and $[Mo(Ntol)_2(O\text{-}t\text{-}Bu)_2]_2$ display asymmetrically bridging organoimido ligands. For two different descriptions of the bonding in these species, see the following: (a) Thorn, D. L.; Nugent, W. A.; Harlow, R. L. *J. Am. Chem. Soc.* **1981**, *103*, 357. (b) Chisholm, M. H.; Folting, K. F.; Huffman, J. C.; Ratermann, A. L. *Inorg. Chem.* **1982**, *21*, 978.

(19) (a) Ramsey, N. F. *Phys. Rev.* **1950**, *78*, 699. (b) Griffith, J. S.; Orgel, L. E. *Trans. Faraday Soc.* **1957**, *53*, 601.

(20) Nakano, T. *Bull. Chem. Soc. Jpn.* **1977**, *50*, 661.

(21) Figgis, B. N.; Kidd, R. G.; Nyholm, R. S. *Proc. R. Soc. London, A* **1962**, *269*, 469.

(22) Carrington, A. *Mol. Phys.* **1960**, *3*, 271.

(23) Figgis, B. N. *Introduction to Ligand Fields*; Wiley: New York, 1966; pp 248–259.

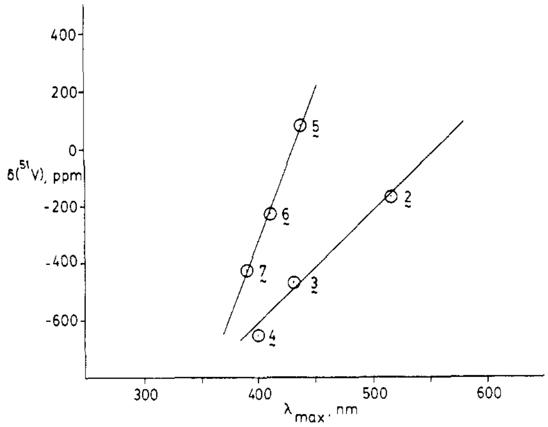

Figure 2. Correlation of $\delta(^{51}V)$ with visible region λ_{max}. See text for numbering scheme.

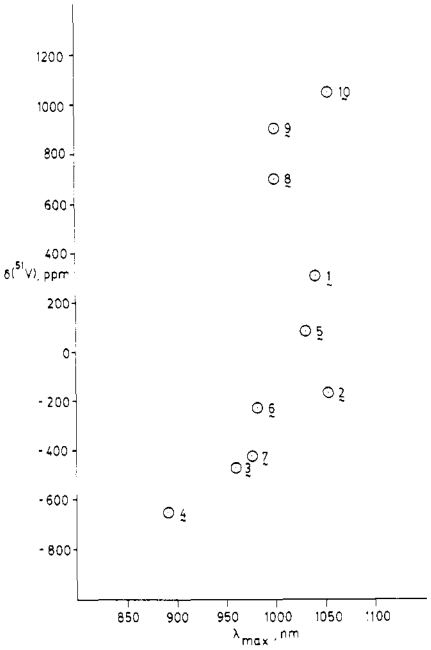

Figure 3. Correlation of $\delta(^{51}V)$ with near-IR region λ_{max}. See text for numbering scheme.

Equation 10 assumes that the metal orbitals are "pure" d orbitals (i.e., the effects of covalent character in the metal–ligand bonds have been ignored); covalent bond character can be accounted for by including in eq 10 a term that specifies the extent of d-orbital participation in the molecular orbitals of interest. This can be done by including either a k^2 term (where k is the orbital reduction factor as defined by Griffith[24]) or a C^2 term (where C is the d-orbital coefficient of the appropriate molecular orbital).[20,25] Thus, the expression to be used herein for σ_{para} is shown in eq 11.[26]

$$\sigma_{\text{para}} = -(\text{constant})\sum_i C_0{}^2 C_i{}^2 (E_i - E_0)^{-1} r^{-3} \qquad (11)$$

The dependence of $\delta(^{51}V)$ upon $(\Delta E)^{-1}$ for the family of V(Ntol)X_3 compounds is presented graphically in Figure 2 (for the visible region transition) and in Figure 3 (for the near-IR region transition). In Figure 2, two lines with different slopes are obtained for the series of *tert*-butoxide complexes (**2**–**4**) and the 2,6-dimethylphenoxide complexes (**5**–**7**); when analogous pairs in these series are compared, it is seen that while a given aryloxide species displays a higher energy visible region transition than its alkoxide counterpart, the corresponding $\delta(^{51}V)$ value for the aryloxide species lies *downfield* of that shown by the *tert*-butoxide analogue. This disparity likely reflects significant differences in the (C^2r^{-3}) terms (eq 11) for the two series, which alter the dominance of the (ΔE^{-1}) factor in the paramagnetic shielding expression. At this stage, further speculations on this point would seem to be unwise, especially in view of the five-coordinate nature of the aryloxide complexes **5** and **6** vis-à-vis the four-coordinate nature of their *tert*-butoxide counterparts **2** and **3** (note the significant downfield chemical shifts induced by coordination of THF or PPh_3 to V(Ntol)Cl_3 as given in Table II). In spite of these uncertainties, Figure 2 illustrates that successive replacement of Cl by more electronegative oxygen donors (O-*t*-Bu or OAr) induces a progressive shift of ΔE_{vis} to higher energy, thus diminishing the contribution of σ_{para} and leading to higher field ^{51}V chemical shifts. In contrast, there is no apparent correlation of the basal ligand set's electronegativity with the magnitude of $\Delta E_{near\text{-}IR}$ as depicted in Figure 3.

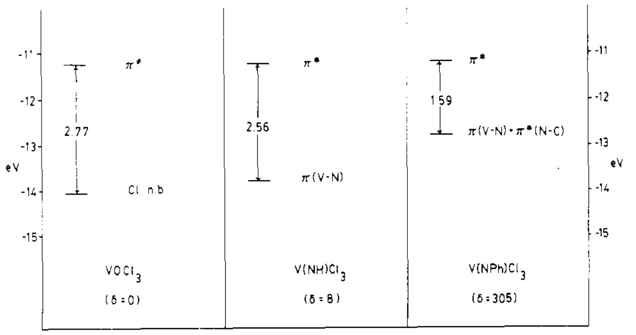

Figure 4. HOMO–LUMO transition energies for $VOCl_3$, V(NH)Cl_3, and V(NPh)Cl_3 as obtained from extended Hückel calculations. ^{51}V chemical shift values shown in parentheses are experimentally determined values for $VOCl_3$, V(N-*t*-Bu)Cl_3,[1h] and V(Ntol)Cl_3.

In order to better understand the nature of the observed electronic transitions and their influence on $\delta(^{51}V)$, we have carried out calculations of the extended Hückel type[27] on several complexes. We first set out to address the question of why the ^{51}V chemical shifts of (*t*-BuN)VCl_3 (δ +8) and (*i*-PrN)VCl_3 (δ +21)[1h] should mimic that of $OVCl_3$ (δ 0) and differ so considerably from that of V(Ntol)Cl_3 (δ +305). To that end, EHMO calculations were performed on $OVCl_3$, V(NPh)Cl_3, and V(NH)Cl_3 (used to model the above alkylimido complexes). The salient portion of the results is presented in Figure 4, which depicts the calculated energies of the HOMO and LUMO for each species. It is seen that the LUMO energies do not vary appreciably among the three complexes; these doubly degenerate orbitals are primarily V–N (or V–O) π antibonding in character, with a significant admixture of $d_{x^2-y^2}$ and d_{xy}. In the case of V(NPh)Cl_3, the LUMO energy shown in the figure is an average of two closely spaced orbitals rendered nondegenerate by the C_s symmetry imposed by the planar phenylimido group. The key differences among the three complexes are found in the constitutions and energies of their HOMOs. The HOMO in both V(NH)Cl_3 and V(NPh)Cl_3 is primarily V–N π bonding in character. However, in the case of V(NPh)Cl_3, the HOMO also contains a considerable N–C(aryl) π^* component, which is not possible for the NH or alkylimido complexes. The incorporation of this antibonding component thus destabilizes the HOMO of V(NPh)Cl_3, thereby reducing ΔE, increasing the σ_{para} contribution, and driving the ^{51}V chemical shift to lower field. Also apparent in Figure 4 is the close congruence in the calculated HOMO–LUMO transition energies for $VOCl_3$ and V(NH)Cl_3, which accords with the similarities in $\delta(^{51}V)$ for $VOCl_3$ and the aforementioned (alkylimido)vanadium trichlorides.

---

[24] Griffith, J. S. *The Theory of Transition Metal Ions*; Cambridge University: London, 1961; pp 284–285.

[25] Rehder, D.; Bechtold, H.-C.; Kecici, A.; Schmidt, H.; Siewing, M. *Z. Naturforsch., B: Anorg. Chem., Org. Chem.* **1982**, *37B*, 631.

[26] Implicit in eq 11 is the assumption that vanadium 4p orbitals do not participate to a significant extent in the states of interest. This assumption is commonly made,[14] and our calculations confirm that these orbitals make a negligible contribution to the molecular orbitals in the frontier region.

[27] (a) Hoffmann, R. *J. Chem. Phys.* **1963**, *39*, 1397. (b) Ammeter, J. H.; Bürgi, H.-B.; Thibeault, J. C.; Hoffmann, R. *J. Am. Chem. Soc.* **1978**, *100*, 3686.

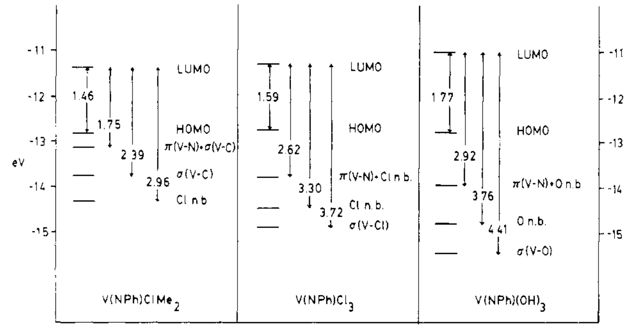

Figure 5. Selected transition energies for $V(NPh)ClMe_2$, $V(NPh)Cl_3$, and $V(NPh)(OH)_3$ as obtained from extended Hückel calculations.

We were also interested in the origins of the large ^{51}V chemical shift disparities between the alkyl and alkoxide derivatives of $V(Ntol)Cl_3$ as well as the reason why the (trimethylsilyl)methyl derivatives displayed only a single, broad absorption in their electronic spectra in contrast to the observance of two absorptions for the other $V(Ntol)Cl_3$ derivatives examined. Accordingly, EHMO calculations were carried out on several methyl and hydroxide derivatives of $V(NPh)Cl_3$. Relevant aspects of the calculations on $V(NPh)(OH)_3$, $V(NPh)Cl_3$, and $V(NPh)Me_2Cl$ are presented in Figure 5. For each of these species, the calculated energies of five analogous molecular orbitals are given. As before, the HOMO and LUMO energies shown are averages of two closely spaced levels (A′ and A″ under C_s symmetry), and the constitution of these orbitals is as described above. Note that the HOMO and LUMO energies (and hence the corresponding transition energies) are relatively unaffected by changes in the basal ligand set. This accords nicely with the observed similarities in the energies of the near-IR transition in the electronic spectra of complexes **1**–**10** (Table I) and supports our assignment of this feature as a V–N ($\pi \rightarrow \pi^*$) transition.

Also presented in Figure 5 are energy levels for three orbitals in each complex that involve σ and nonbonding participation by the basal ligands. The energy levels shown are averages for closely grouped orbitals of similar character. Note that, as expected, the energies of these orbitals vary greatly depending upon the electronegativity (or valence atomic orbital energy) of the basal ligand donor atom. In the case of $V(NPh)ClMe_2$, the energy of the upper σ level approaches that of the HOMO, consistent with our observation of only a single, broad absorption in the near-IR region for the (trimethylsilyl)methyl complexes **8**–**10**. Analogous orbitals in the $V(NPh)Cl_3$ and $V(NPh)(OH)_3$ species lie at much lower energies, consistent with our observations of well-resolved absorptions in the electronic spectra of complexes **1**–**7**.

Hence, two types of electronic transitions are influencing the paramagnetic shielding term for (arylimido)vanadium(V) complexes, and it is the magnitude of the energy difference between these transitions that ultimately determines the ^{51}V chemical shift of these species. The first of these is a low-energy transition in the near-IR region, associated with the V–N multiple bond, and is approximately energy invariant in all of the complexes studied. This transition imparts a large deshielding contribution to the vanadium nucleus. The second type of transition involves electrons associated with the basal ligands. The energies of these ($\sigma \rightarrow \pi^*$) and ($n \rightarrow \pi^*$) transitions increase considerably as the electronegativity of the basal ligand donor atoms increases. As the energy of these transitions increase, the overall paramagnetic shielding experienced by the vanadium atom must decrease, and the resulting ^{51}V NMR resonance moves to higher field.

Experimental Section

All reactions and manipulations were performed either in vacuo or under an atmosphere of dry nitrogen. Solvents employed were dried by refluxing in the presence of appropriate reagents, distilled, and introduced into the reaction vessels by vacuum transfer. $Mg(CH_2SiMe_3)_2$[28] and $C_5H_5SiMe_3$[29] were prepared as described in the literature. Infrared spectra were recorded as Nujol mulls on a Perkin-Elmer 1330 spectrophotometer and were calibrated with the use of a polystyrene film. ^1H (400.1-MHz) and ^{51}V (105.2-MHz) NMR spectra were obtained on an IBM/Bruker WM-400 instrument at 25 °C and are referenced to Me_4Si and $OVCl_3$, respectively. Electronic spectra in the visible and near-IR regions were recorded with a Cary 14 spectrophotometer. Elemental analyses were performed by Galbraith Laboratories.

Preparation of $V(Ntol)Cl_3$. A portion of $VOCl_3$ (10.5 mL, 111.5 mol) was syringed into a 250-mL flask bearing a reflux condenser and containing a solution of *p*-tolyl isocyanate (14 mL, 111 mmol) in octane (80 mL). The mixture was refluxed under N_2 (1 atm) for 3 h, during which time the solution acquired a rich emerald green color. The solution was then taken to dryness, leaving a dark purple solid, which was dried in vacuo at 70 °C for 18 h to remove traces of unreacted starting materials. Although the resultant purple-black solid is entirely satisfactory for use in subsequent reactions, analytically pure samples may be obtained by sublimation (110 °C (10^{-4} Torr)) onto a water-cooled probe, yielding the product as glistening purple-black needles in ca. 90% yield. Anal. Calcd for $C_7H_7Cl_3NV$: C, 32.04; H, 2.69; N, 5.34. Found: C, 32.25; H, 2.91; N, 5.62. ^1H NMR ($CDCl_3$): δ 7.33 (AB q, J_{AB} = 7.8 Hz, 4 H, $C_6\mathit{H}_4CH_3$), 2.53 (s, 3 H, $C\mathit{H}_3$). ^{51}V NMR ($CDCl_3$): δ 305 (fwhm = 500 Hz). λ_{max} ($CH_3C_6H_5$): 654, 1040 nm.

Preparation of (p-$XC_6H_4N)VCl_3$ (X = F, Cl, Br, OCH_3, CF_3). The following procedure for the synthesis of (p-$ClC_6H_4N)VCl_3$ may be applied to the preparation of any of the para-substituted arylimido derivatives above. All compounds displayed mass spectra consistent with their formulations. A portion of $VOCl_3$ (0.54 g, 3.1 mmol) was added to a solution of *p*-chlorophenyl isocyanate (0.46 g, 3.0 mmol) in octane (50 mL). The mixture was refluxed under an atmosphere of N_2 for 16 h, and solvent was then removed in vacuo. The dark brown solid product was triturated with pentane (2 × 40 mL), collected by filtration, and dried in vacuo. ^1H NMR ($CDCl_3$): δ 7.43 (AB q, J_{AB} = 8.0 Hz). ^{51}V NMR ($CDCl_3$): δ 253 (fwhm = 525 Hz).

(p-$CH_3OC_6H_4N)VCl_3$. ^1H NMR ($CDCl_3$): δ 7.24 (AB q, J_{AB} = 8.8 Hz, 4 H, $C_6\mathit{H}_4OCH_3$), 3.91 (s, 3 H, $C\mathit{H}_3$). ^{51}V NMR ($CDCl_3$): δ 403 (fwhm = 730 Hz).

(p-$FC_6H_4N)VCl_3$. ^1H NMR ($CDCl_3$): δ 7.60 (br t, 2 H), 7.08 (br t, 2 H). ^{51}V NMR ($CDCl_3$): δ 258 (fwhm = 370 Hz).

(p-$F_3CC_6H_4N)VCl_3$. ^1H NMR ($CDCl_3$): δ 7.71 (br). ^{51}V NMR ($CDCl_3$): δ 182 (fwhm = 500 Hz).

(p-$BrC_6H_4N)VCl_3$. ^1H NMR ($CDCl_3$): δ 6.41 (AB q, J_{AB} = 7.9 Hz). ^{51}V NMR ($CDCl_3$): δ 251 (fwhm = 610 Hz).

Preparation of $V(Ntol)Cl_3(THF)$. A portion of $V(Ntol)Cl_3$ (0.50 g, 1.91 mmol) was dissolved in THF (20 mL), affording a golden solution. Hexane (ca. 5 mL) was distilled in, and the solution was cooled to 0 °C for 1 h, causing the deposition of violet crystals. The solid was collected by filtration, and upon being dried in vacuo, the product was obtained as orange microcrystals. Anal. Calcd for $C_{11}H_{15}NOCl_3V$: C, 39.49; H, 4.52; N, 4.19. Found: C, 39.48; H, 4.63; N, 4.15. ^1H NMR ($CDCl_3$): δ 7.42 (AB q, J_{AB} = 8.3 Hz, 4H, $C_6\mathit{H}_4CH_3$), 4.34 (t, 4 H, $OC\mathit{H}_2(CH_2)_2C\mathit{H}_2$), 2.55 (s, 3 H, $C_6H_4C\mathit{H}_3$), 2.06 (quintet, 4 H, $OCH_2(C\mathit{H}_2)_2CH_2$). ^{51}V NMR ($CDCl_3$): δ 374 (fwhm = 1900 Hz).

Preparation of $V(Ntol)Cl_3(PPh_3)$. A portion of $V(Ntol)Cl_3$ (0.97 g, 3.7 mmol) was added to a solution of PPh_3 (0.97 g, 3.7 mmol) in CH_2Cl_2 (30 mL). The resulting copper-colored solution was stirred at room temperature for 1 h, and the solution was concentrated by evaporation to ca. 20 mL. The solution was chilled to 0 °C, and hexane (ca. 5 mL) was admitted via distillation, causing the deposition of bronze microcrystals, which were collected by filtration and dried in vacuo to give the product as a khaki powder. Anal. Calcd for $C_{25}H_{22}NPCl_3V$: C, 57.22; H, 4.23; N, 2.67. Found: C, 57.43; H, 4.46; N, 2.69. ^1H NMR ($CDCl_3$): δ 7.65–7.38 (m, 15 H, $P(C_6\mathit{H}_5)_3$), 7.13 (AB q, J_{AB} = 8.2 Hz, 4 H, $C_6\mathit{H}_4CH_3$), 2.47 (s, 3 H, $C_6H_4C\mathit{H}_3$). ^{51}V NMR ($CDCl_3$): δ 392 (fwhm = 700 Hz).

Preparation of $V(Ntol)Cl_2(O$-t-$Bu)$. A portion of KO-*t*-Bu (0.43 g, 3.8 mmol) was added to a stirred solution of $V(Ntol)Cl_3$ (1.0 g, 3.8 mmol) in THF (30 mL) at room temperature, affording a blood red solution. After 1 h, the solvent was removed in vacuo, leaving a dark purple, gummy residue, which was triturated with CH_2Cl_2 (25 mL) and filtered through a Celite pad. The filtrate was taken to dryness, and the residue was triturated with a minimum amount of pentane. The dark purple solid product was collected by filtration and dried in vacuo. Anal. Calcd for $C_{11}H_{16}NOCl_2V$: C, 44.03; H, 5.37; N, 4.67. Found: C, 44.26; H, 5.33; N, 4.80. ^1H NMR ($CDCl_3$): δ 7.19 (AB q, J_{AB} = 8.2 Hz, 4 H, $C_6\mathit{H}_4CH_3$), 2.42 (s, 3 H, $C_6H_4C\mathit{H}_3$), 1.61 (s, 9 H, $OC(CH_3)_3$). ^{51}V

---

[28] Andersen, R. A.; Wilkinson, G. *J. Chem. Soc., Dalton Trans.* **1977**, 809.

[29] Kraihanzel, C. S.; Losee, M. L. *J. Am. Chem. Soc.* **1968**, *90*, 4701.

($\mathrm{CDCl_3}$): δ −171 (fwhm = 500 Hz). $\lambda_{\max}$ ($\mathrm{C_6H_5CH_3}$): 516, 1052 nm.

Preparation of V(Ntol)Cl(O-*t*-Bu)$_2$. A portion of KO-*t*-Bu (0.86 g, 7.6 mmol) was added to a stirred solution of V(Ntol)Cl$_3$ (1.0 g, 3.8 mmol) in THF (40 mL) at room temperature. After 5 h, the solvent was removed in vacuo, and the residue was triturated with hexane (40 mL). Filtration through a Celite pad and evaporation of the filtrate yielded the bright orange solid product, which, if desired, may be sublimed (70 °C (10^{-4} Torr)) to produce orange crystals. Anal. Calcd for $\mathrm{C_{15}H_{25}NO_2ClV}$: C, 53.34; H, 7.46; N, 4.15. Found: C, 53.29; H, 7.49; N, 4.59. ^{1}H NMR ($\mathrm{CDCl_3}$): δ 7.11 (AB q, J_{AB} = 8.3 Hz, 4 H, $\mathrm{C_6\mathit{H}_4CH_3}$), 2.36 (s, 3 H, $\mathrm{C_6H_4C\mathit{H}_3}$), 1.50 (s, 18 H, $\mathrm{OC(CH_3)_3}$). ^{51}V NMR ($\mathrm{CDCl_3}$): δ −472 (fwhm = 390 Hz). $\lambda_{\max}$ ($\mathrm{CH_3C_6H_5}$): 432, 960 nm.

Preparation of V(Ntol)(O-*t*-Bu)$_3$. A portion of KO-*t*-Bu (1.3 g, 11.6 mmol) was added to a stirred solution of V(Ntol)Cl$_3$ (1.0 g, 3.8 mmol) in THF (40 mL) and the resultant mixture warmed to 55 °C for 1.5 h. The reaction was stirred an additional 12 h at room temperature, and the solvent was removed in vacuo, leaving an orange-yellow slightly tacky residue. This material was triturated with hexane (ca. 30 mL), and the solution was filtered through a Celite pad. The filtrate was evaporated to dryness, yielding the product as a yellow-orange solid. Anal. Calcd for $\mathrm{C_{19}H_{34}NO_3V}$: C, 60.79; H, 9.13; N, 3.73. Found: C, 60.93; H, 9.05; N, 3.90. ^{1}H NMR ($\mathrm{CDCl_3}$): δ 7.08 (AB q, J_{AB} = 8.3 Hz, 4 H, $\mathrm{C_6\mathit{H}_4CH_3}$), 2.33 (s, 3 H, $\mathrm{C_6H_4C\mathit{H}_3}$), 1.42 (s, 27 H, $\mathrm{OC(CH_3)_3}$). ^{51}V NMR ($\mathrm{CDCl_3}$): δ −654 (fully resolved 1:1:1 t, $J_{^{51}\mathrm{V}-^{14}\mathrm{N}}$ = 111 Hz) (fwhm = 90 Hz). $\lambda_{\max}$ ($\mathrm{C_6H_5CH_3}$): 399, 891 nm.

Preparation of V(Ntol)Cl$_2$(OC$_6$H$_3$(CH$_3$)$_2$)(THF). A portion of 2,6-dimethylphenol (0.14 g, 1.14 mmol) was added to a stirred solution of V(Ntol)Cl$_3$ (0.30 g, 1.14 mmol) in THF (ca. 50 mL) at room temperature. After the mixture was stirred for 20 min, the solvent was removed in vacuo. The residue was dissolved in pentane (30 mL) and filtered, and the filtrate was evaporated to dryness, yielding the product as a dark purple solid. ^{1}H NMR ($\mathrm{C_6D_6}$): δ 6.87 (d, J = 7.2 Hz, 2 H, phenoxide meta protons), 6.80 (t, J = 7.2 Hz, 1 H, phenoxide para proton), 6.52 (AB q, J_{AB} = 7.9 Hz, 4 H, $\mathrm{C_6\mathit{H}_4CH_3}$), 3.99 (m, 4 H, $\overline{\mathrm{OC\mathit{H}_2(CH_2)_2C\mathit{H}_2}}$), 2.30 (s, 6 H, $\mathrm{OC_6H_3(C\mathit{H}_3)_2}$), 1.73 (s, 3 H, $\mathrm{C_6H_4C\mathit{H}_3}$), 1.42 (m, 4 H, $\overline{\mathrm{OCH_2(C\mathit{H}_2)_2CH_2}}$). ^{51}V NMR ($\mathrm{CDCl_3}$): δ 77 (fwhm = 1170 Hz). $\lambda_{\max}$ ($\mathrm{C_6H_5CH_3}$): 434, 1028 nm.

Preparation of [V(Ntol)Cl(OC$_6$H$_3$(CH$_3$)$_2$)$_2$]$_2$. A portion of 2,6-dimethylphenol (0.56 g, 4.6 mmol) was added to a stirred solution of V(Ntol)Cl$_3$ (0.40 g, 1.5 mmol) in THF (50 mL) at room temperature. After 14 h, solvent was removed and the residue was extracted with pentane (ca. 40 mL). After filtration, the pentane extract was concentrated to ca. 25-mL volume and cooled at 0 °C for 12 h. The dark red crystalline plates of the product were collected by filtration and dried in vacuo. ^{1}H NMR ($\mathrm{C_6D_6}$): δ 6.90 (d, J = 7.2 Hz, 4 H, phenoxide meta protons), 6.80 (t, J = 7.2 Hz, 2 H, phenoxide para protons), 6.38 (AB q, J_{AB} = 7.4 Hz, $\mathrm{C_6\mathit{H}_4CH_3}$), 2.42 (s, 12 H, $\mathrm{OC_6H_3(C\mathit{H}_3)_2}$), 1.70 (s, 3 H, $\mathrm{C_6H_4C\mathit{H}_3}$). ^{51}V NMR ($\mathrm{CDCl_3}$): δ −231 (fwhm = 463 Hz). $\lambda_{\max}$ ($\mathrm{C_6H_5CH_3}$): 411, 980 nm.

Preparation of V(Ntol)(OC$_6$H$_3$(CH$_3$)$_2$)$_3$. A portion of 2,6-dimethylphenol (0.84 g, 6.9 mmol) was added to a stirred solution of V(Ntol)Cl$_3$ (0.6 g, 2.3 mmol) and Et$_3$N (1.0 g, 9.9 mmol) in THF (60 mL). After 2 h, solvent was removed in vacuo and the residue was extracted into pentane (ca. 40 mL). After filtration, the pentane was removed in vacuo, leaving the product as a deep orange oil. Anal. Calcd for $\mathrm{C_{31}H_{34}NO_3V}$: C, 71.66; H, 6.60; N, 2.70. Found: C, 70.52; H, 6.55; N, 2.46. ^{1}H NMR ($\mathrm{C_6D_6}$): δ 6.96 (d, J = 7.4 Hz, 6 H, phenoxide meta protons), 6.82 (t, J = 7.4 Hz, 3 H, phenoxide para protons), 6.37 (AB q, J_{AB} = 8.2 Hz, $\mathrm{C_6\mathit{H}_4CH_3}$), 2.45 (s, 18 H, $\mathrm{OC_6H_3(C\mathit{H}_3)_2}$), 1.73 (s, 3 H, $\mathrm{C_6H_4C\mathit{H}_3}$). ^{51}V NMR: δ −428 (partially resolved t, $J_{^{51}\mathrm{V}-^{14}\mathrm{N}}$ = 98 Hz) (fwhm = 366 Hz). $\lambda_{\max}$ ($\mathrm{C_6H_5CH_3}$): 390, 977 nm.

Preparation of (η^5-C$_5$H$_5$)V(Ntol)Cl$_2$. A solution of $\mathrm{C_5H_5SiMe_3}$ (0.63 g, 4.6 mmol) in $\mathrm{CH_2Cl_2}$ (10 mL) was slowly added to a stirred solution of V(Ntol)Cl$_3$ (1.1 g, 4.3 mmol) in $\mathrm{CH_2Cl_2}$ (60 mL). The reaction vessel was placed in a 50 °C water bath, and the contents were stirred for 14 h. The resultant golden brown solution was cooled to room temperature, filtered, and evaporated to dryness. The residue was triturated with hexane (ca. 30 mL), and the black microcrystalline product was collected by filtration and dried in vacuo. Anal. Calcd for $\mathrm{C_{12}H_{12}NCl_2V}$: C, 49.34; H, 4.15; N, 4.80. Found: C, 46.63; H, 4.53; N, 4.82. ^{1}H NMR ($\mathrm{CDCl_3}$): δ 7.13 (AB q, J_{AB} = 7.0 Hz, 4 H, $\mathrm{C_6\mathit{H}_4CH_3}$), 6.58 (s, 5 H, $\mathrm{C_5H_5}$), 2.44 (s, 3 H, $\mathrm{C_6H_4C\mathit{H}_3}$). ^{51}V NMR ($\mathrm{CDCl_3}$): δ −240 (fwhm = 790 Hz).

Preparation of V(Ntol)Cl$_2$(CH$_2$SiMe$_3$). A portion of $\mathrm{Mg(CH_2SiMe_3)_2}$ (0.11 g, 0.55 mmol) was added to a stirred solution of V(Ntol)Cl$_3$ (0.6 g, 2.3 mmol) in toluene (50 mL) at 0 °C. After 20 min, the solvent was removed in vacuo. The residue was triturated with pentane (ca. 25 mL) and filtered. Evaporation of the filtrate left the product as a tacky orange solid. Noticeable decomposition occurs within hours at room temperature. Some $\mathrm{V(Ntol)Cl(CH_2SiMe_3)_2}$ is usually present as a minor impurity. ^{1}H NMR ($\mathrm{C_6D_6}$): δ 6.95 (AB q, J_{AB} = 8.0 Hz, 4 H, $\mathrm{C_6\mathit{H}_4CH_3}$), 4.71 (br, fwhm = 13.3 Hz, 2 H, $\mathrm{C\mathit{H}_2Si(CH_3)_3}$), 1.92 (s, 3 H, $\mathrm{C_6H_4C\mathit{H}_3}$), 0.02 (s, 9 H, $\mathrm{CH_2Si(C\mathit{H}_3)_3}$). ^{51}V NMR ($\mathrm{C_6D_6}$): δ 697 (fwhm = 378 Hz). $\lambda_{\max}$ ($\mathrm{CH_3C_6H_5}$): 1000 nm.

Preparation of V(Ntol)Cl(CH$_2$SiMe$_3$)$_2$. A portion of $\mathrm{Mg(CH_2SiMe_3)_2}$ (0.15 g, 0.75 mmol) was added to a stirred solution of V(Ntol)Cl$_3$ (0.4 g, 1.5 mmol) in toluene (50 mL) maintained at 0 °C with the use of an ice–water bath. The solution was allowed to warm to room temperature over a 2-h period, whereupon the solvent was removed in vacuo. The residue was extracted into pentane (ca. 40 mL) and filtered. The filtrate was taken to dryness, yielding the product as a bright orange oil, which decomposes over a period of several days. The product is usually contaminated with minor amounts of $\mathrm{V(Ntol)(CH_2SiMe_3)_3}$. ^{1}H NMR ($\mathrm{C_6D_6}$): δ 7.14 (AB q, J_{AB} = 8.5 Hz, $\mathrm{C_6\mathit{H}_4CH_3}$), 3.43 (s br, fwhm = 27 Hz, 2 H, $\mathrm{C\mathit{H}_2Si(CH_3)_3}$), 2.28 (s br, fwhm = 27 Hz, 2 H, $\mathrm{C\mathit{H}_2Si(CH_3)_3}$), 2.00 (s, 3 H, $\mathrm{C_6H_4C\mathit{H}_3}$), 0.10 (s, 18 H, $\mathrm{CH_2Si(C\mathit{H}_3)_3}$). ^{51}V NMR ($\mathrm{C_6D_6}$): δ 900 (fwhm = 353 Hz). $\lambda_{\max}$ ($\mathrm{CH_3C_6H_5}$): 1000 nm.

Preparation of V(Ntol)(CH$_2$SiMe$_3$)$_3$. A portion of $\mathrm{Mg(CH_2SiMe_3)_2}$ (0.54 g, 2.7 mmol) was added to a stirred solution of V(Ntol)Cl$_3$ (0.48 g, 1.8 mmol) in toluene (50 mL) at 0 °C. The solution was allowed to warm to room temperature over a 3-h period, whereupon the toluene was removed in vacuo. The product was extracted into pentane (ca. 40 mL) and filtered, and the pentane was removed in vacuo, affording the product as an orange oil, which decomposes over a period of ca. 1 month. Anal. Calcd for $\mathrm{C_{19}H_{40}NSi_3V}$: C, 54.63; H, 9.65; N, 3.35. Found: C, 53.49; H, 8.58; N, 3.77. ^{1}H NMR ($\mathrm{C_6D_6}$): δ 7.25 (AB q, J_{AB} = 8.1 Hz, 4 H, $\mathrm{C_6\mathit{H}_4CH_3}$), 2.08 (s, 3 H, $\mathrm{C_6H_4C\mathit{H}_3}$), 1.84 (br, fwhm = 53 Hz, 6 H, $\mathrm{C\mathit{H}_2Si(CH_3)_3}$), 0.13 (s, 27 H, $\mathrm{CH_2Si(C\mathit{H}_3)_3}$). ^{51}V NMR ($\mathrm{C_6D_6}$): δ 1046 (partially resolved t, $J_{^{51}\mathrm{V}-^{14}\mathrm{N}}$ = 94 Hz) (fwhm = 270 Hz). $\lambda_{\max}$ ($\mathrm{CH_3C_6H_5}$): 1055 nm.

Hydrolysis of V(Ntol)(OC$_6$H$_3$(CH$_3$)$_2$)$_3$. A portion of $\mathrm{V(Ntol)(OC_6H_3(CH_3)_2)_3}$ (0.011 g, 2.1×10^{-2} mmol) was introduced into an NMR tube, dissolved in $\mathrm{C_6D_6}$, and fitted with a septum cap. A total of 0.38 μL of $\mathrm{H_2O}$ (2.1×10^{-2} mmol) was introduced into the tube with a syringe, causing an immediate reaction. The ^{1}H NMR spectrum of the reaction mixture displayed resonances due to $\mathrm{VO(OC_6H_3(CH_3)_2)_3}$, unreacted $\mathrm{V(Ntol)(OC_6H_3(CH_3)_2)_3}$, 2,6-dimethylphenol, and *p*-toluidine in the ratio 2:1:2:2. The following NMR data refer to $\mathrm{VO(OC_6H_3(CH_3)_2)_3}$. ^{1}H NMR ($\mathrm{C_6D_6}$): δ 6.86 (d, J = 7.5 Hz, 6 H, phenoxide meta protons), 6.76 (t, J = 7.5 Hz, 3 H, phenoxide para protons), 2.37 (s, 18 H, $\mathrm{OC_6H_3(C\mathit{H}_3)_2}$). ^{51}V NMR ($\mathrm{C_6D_6}$): δ −511 (fwhm = 20 Hz).

Crystallographic Study. Crystals of $\mathrm{[V(Ntol)Cl(O\text{-}2,6\text{-}C_6H_3(CH_3)_2]_2}$ were obtained by cooling a saturated pentane solution to ca. −5 °C. A plate of approximate dimensions 0.5 × 0.3 × 0.1 mm was mounted in a glass capillary under an $\mathrm{N_2}$ atmosphere. Preliminary scans indicated a monoclinic space group with systematic absences characteristic of either *I*2/*a* or *I*2/*c*. The *I*2/*c* setting was confirmed by a Patterson map. Accurate cell dimensions were obtained by a least-squares refinement of the angular positions of 15 reflections with $2\theta > 25°$. Intensity measurements were made on a Syntex P2$_1$ diffractometer with graphite (002) monochromatized Mo Kα radiation (λ = 0.71069 Å). A correction was applied for a small amount of decay observed in the intensities of two standard reflections throughout the period of data collection. Intensities were corrected for absorption[30] and Lorentz–polarization factors. Reflections with $I_0 < 0.2\sigma(I_0)$ were reset to $I_0 = 0.2\sigma(I_0)$. All unique data were used in the subsequent refinement.

The structure was solved by the heavy-atom method. All hydrogen atoms attached to the aryl rings were located in difference maps, but the methyl group hydrogens were not found. Therefore, all hydrogen atoms were placed in idealized positions and were included in structure factor calculations but were not included in the refinement. All positional and anisotropic thermal parameters of the non-hydrogen atoms were refined by full-matrix least-squares procedures. Calculations were performed on a Honeywell 66/6000 computer at the University of Kansas using programs in the DNA system of F. Takusagawa. The quantity minimized was $\sum w(|F_o| - k|F_c|)^2$, where w refers to the weights and k is the scale factor (final value of k = 4.878 (4)). In the early refinements, weights of $w = 4F_o^2/\sigma^2(F_o^2)$ were used. In later refinements, weights were taken as $1/\sigma_{\mathrm{new}}^2$, where $\sigma_{\mathrm{new}}^2 = \sigma^2 + 0.5A|F_o|^2 + 0.5B[(\sin\theta)/\lambda]^2$; the values of A and B were obtained by least-squares minimization of the functions $\sum(\Delta F^2 - \sigma_{\mathrm{new}}^2)^2$ for 20 separate segments in $|F_o|$ and $(\sin\theta)/\lambda$. Atomic scattering factors for all atoms and anomalous dispersion factors for V and Cl were taken from the usual source.[31] A final difference Fourier

---

(30) North, A. C. T.; Phillips, D. C.; Matthews, F. S. *Acta Crystallogr., Sect. A: Cryst. Phys., Diffr., Theor. Gen. Crystallogr.* **1968**, *24*, 351.

(31) Cromer, D. T.; Waber, J. T. *International Tables for X-ray Crystallography*; Kynoch: Birmingham, England, 1974; Vol. IV.

J. Am. Chem. Soc. 1987, 109, 7416-7420

synthesis showed no significant residual electron density; the largest peak was 0.34 e/Å^3. See Table VI for a summary of crystallographic data.

Theoretical Calculations. Calculations were of the extended Hückel type,[27] with programs locally modified and supplied by Prof. Keith Purcell. Values of bond lengths and bond angles employed were taken from structural data.[1d,7,32] The V–C bond length was chosen to be the sum of their covalent radii (1.994 Å), and an N–V–C angle of 106° was assumed. Values of Slater exponents, coefficients, and atomic orbital energies for elements with $Z \leq 17$ were taken from the literature.[27] The Slater exponents (coefficients in parentheses) for vanadium (chosen to be in the +3 oxidation state) were determined[33] to be as follows: 3d, 4.75 (0.498), 1.90 (0.655); 4s, 1.6 (1.0); 4p, 1.6 (1.0). Atomic orbital energies for vanadium (calculated by the method of Gray et al.[34]) employed in the calculations were $H_{dd} = -12.55$ eV, $H_{ss} = -10.74$ eV, and $H_{pp} = -7.04$ eV.

Acknowledgment. This work was supported by the National Science Foundation (Grant CHE-8604359). D.D.D. thanks the Phillips Petroleum Corp. for a fellowship. The WM-400 NMR spectrometer employed in this work was purchased with the assistance of an NSF instrumentation award. We are grateful to Professors K. F. Purcell and P. M. A. Sherwood for their aid in implementing the EHMO calculations.

Supplementary Material Available: Tables of fractional coordinates of hydrogen atoms, anisotropic thermal parameters, complete bond distances and angles, and torsion angles (8 pages); listing of observed and calculated structure factor amplitudes (14 pages). Ordering information is given on any current masthead page.

---

(32) (a) Scherfise, K. D.; Dehnicke, K.; Schweda, E. *Z. Anorg. Allg. Chem.* **1985**, *528*, 117. (b) Karakda, K.; Kuchitsu, K. *Inorg. Chim. Acta* **1975**, *13*, 113.

(33) Richardson, J. W.; Niewport, W. C.; Powell, R. R.; Edgell, W. F. *J. Chem. Phys.* **1962**, *36*, 1057.

(34) Basch, H.; Viste, A.; Gray, H. B. *Theor. Chim. Acta* **1965**, *3*, 458.

Bridge Deprotonation of *nido*-2,3-RR′$C_2B_4H_6$ Carboranes and B_5H_9: A Kinetic Study

Mark E. Fessler,[1a] Thomas Whelan,[1b] James T. Spencer,[1b] and Russell N. Grimes*

Contribution from the Department of Chemistry, University of Virginia, Charlottesville, Virginia 22901.
Received May 19, 1987

Abstract: The heterogeneous reactions of the title compounds (R = alkyl, arylmethyl, or phenyl; R′ = R or H) with suspended NaH or KH in THF to give $M^+[RR'C_2B_4H_5^-] + H_2$ were studied as a function of temperature, with determination of reaction rates from the rate of formation of H_2. In all cases the kinetic rate law is pseudo-first order with linear plots of $-\ln k_1$ vs. $1/T$, and the rate is independent of the amount of metal hydride present. Reactions with NaD in place of NaH give no detectable incorporation of deuterium into the carborane anion. The main trend observed is a moderate decrease in reaction rate as the sizes of R and R′ are increased, the effect being greatest in the bis(chromiumbenzyl)carborane complex $[(CO)_3CrPhCH_2]_2C_2B_4H_6$. The data are interpreted as reflecting primarily steric inhibition of the reaction by the R groups, except in the diphenyl derivative $Ph_2C_2B_4H_6$ which exhibits very fast reaction rates at the higher temperatures measured (above −40 °C) and anomalously high activation energy (E_a) and low entropy of activation ($\Delta S^{\ddagger}$). In this instance, electron withdrawal by the phenyl groups via resonance and pronounced steric effects by the phenyls are proposed to account for the observed behavior.

A characteristic feature of most open-cage (non-closo) boranes and carboranes, and many of their metal-containing derivatives, is the presence of one or more three-center-bonded B–H–B groups on the open face of the molecule. These bridging hydrogens typically exhibit acidic behavior toward strong Lewis bases and can be removed to generate a conjugate base anion,[2] e.g.

$$B_5H_9 + NaH \rightarrow Na^+B_5H_8^- + H_2 \qquad (1)$$

Rarely, however, can more than one proton per molecule be removed even under forcing conditions. As first shown long ago by Onak and co-workers,[3] the *nido*-carborane 2,3-$C_2B_4H_8$ and its C- and B-substituted derivatives are readily converted to the corresponding monoanion[3,4] (eq 2 and Figure 1). The reactions proceed cleanly and quantitatively, as we have verified from high-resolution (115.8 MHz) ^{11}B NMR spectra of the anions produced.

$$C_2B_4H_8 + M^+H^- \rightarrow M^+C_2B_4H_7^- + H_2 \qquad (2)$$

The neutral carboranes are readily accessible via the base-promoted reaction of B_5H_9 with alkynes[5] and constitute a large carborane family with a steadily increasing role in synthesis.[6] In recent years, studies of C,C′-disubstituted $R_2C_2B_4H_6$ derivatives have disclosed a variety of synthetically useful processes based on these compounds (e.g., metal-induced oxidative fusion to form $R_4C_4B_8H_8$ clusters,[6,7] alkyne incorporation into the cage,[8] and cage expansion[9,10]).

In the course of our research we have prepared, as reagents for synthetic purposes, a number of *nido*-RR′$C_2B_4H_6$ species in

---

(1) (a) Undergraduate research participant, University of Virginia, 1985–1987. (b) Present address: Department of Chemistry, Syracuse University, Syracuse, NY 13244.

(2) Greenwood, N. N. *The Chemistry of Boron*; Pergamon: Oxford, 1973; Chapter 4; and references therein.

(3) (a) Onak, T.; Dunks, G. B. *Inorg. Chem.* **1966**, *5*, 439. (b) Onak, T.; Lockman, G.; Haran, G. *J. Chem. Soc., Dalton Trans.* **1973**, 2115.

(4) Savory, C. G.; Wallbridge, M. G. H. *J. Chem. Soc., Dalton Trans.* **1974**, 880.

(5) (a) Onak, T. P.; Williams, R. E.; Weiss, H. G. *J. Am. Chem. Soc.* **1962**, *84*, 2830. (b) Hosmane, N. S.; Grimes, R. N. *Inorg. Chem.* **1979**, *18*, 3294. (c) Maynard, R. B.; Borodinsky, L.; Grimes, R. N. *Inorg. Synth.* **1983**, *22*, 211.

(6) (a) Grimes, R. N. *Pure Appl. Chem.* **1987**, *59*, 847. (b) Spencer, J. T.; Pourian, M. R.; Butcher, R. J.; Sinn, E.; Grimes, R. N. *Organometallics* **1987**, *6*, 335 and references therein.

(7) Grimes, R. N. *Adv. Inorg. Radiochem.* **1983**, *26*, 55 and references therein.

(8) Mirabelli, M. G. L.; Sneddon, L. G. *Organometallics* **1986**, *5*, 1510.

(9) Wermer, J. R.; Hosmane, N. S.; Alexander, J. J.; Siriwardane, U.; Shore, S. G. *Inorg. Chem.* **1986**, *25*, 4351.

(10) Beck, J. S.; Kahn, A. P.; Sneddon, L. G. *Organometallics* **1986**, *6*, 2552.

0002-7863/87/1509-7416$01.50/0 © 1987 American Chemical Society